Available online at www.sciencedirect.com
SCIENCE DIRECT®

Journal of the European Ceramic Society 24 (2004) 2319–2327

www.elsevier.com/locate/jeurceramsoc

# Leaching behaviour of silicon nitride materials in sulphuric acid containing KF

J. Schilm*, M. Herrmann, G. Michael

*Fraunhofer Institut für keramische Technologien und Sinterwerkstoffe, Winterberg Str. 28, 01277 Dresden, Germany*

Received 16 May 2002; received in revised form 15 July 2003; accepted 19 July 2003

**Abstract**

The leaching behaviour of gas-pressure-sintered silicon nitride materials with different grain boundary phases was studied in 1 N sulphuric acid at 90 °C with varying additions of KF. The progress of corrosion was investigated in terms of mass loss and thickness of the corroded layer. Also SEM micrographs were taken from the samples and EDX analyses were conducted upon the corroded samples. The corrosion resistance of the materials was found to be sensitive to KF additions as small as 0.01 wt.%. The formation of different corroded sublayers caused by different leaching rates of the single components of the grain boundary phases was shown. It was found that the corrosion behaviour depends strongly on the composition of the grain boundary phase.


*Keywords:* Acid corrosion; Corrosion; Grain boundaries; Leaching; $Si_3N_4$

## 1. Introduction

Silicon nitride, a typical structural ceramic with superior mechanical properties and a high chemical stability, has found many applications in severe corrosive environments. It has been successfully applied in the chemical industry in several components, including bearings, valves and other armatures. Therefore silicon nitride ceramics find applications in environments such as acidic or basic solutions at various temperatures. Although ceramics are generally more stable in corrosive environments than common metal-based materials are, their chemical resistance should be evaluated under these highly corrosive conditions. The corrosive behaviour of silicon nitride materials in several acids, including HF, has been the object of different studies.[1–9] As far as we are aware no information could be found concerning the corrosion behaviour in acids which contain small amounts of highly corrosive $F^-$ ions. It can be expected that no other ionic additive exhibits a more intensive corrosive behaviour than fluoride does. It is of course well known that silica containing glasses and ceramics, especially their grain boundary phases, often exhibit a rather low stability in hydrofluoric acid. The corrosion behaviour of $Si_3N_4$-materials in acids like HCl, $HNO_3$, $H_2SO_4$ or organic acids is different from that in HF. In the acids mentioned first, corrosion of silicon nitride ceramics occurs mainly along the triple junctions.[10,11] The glass network modifying ions like $Mg^{2+}$, $Al^{3+}$ and $Y^{3+}$ are leached by the acid, the network building ions like silicon remain partially inside the corroded triple junctions. Furthermore the thin films with a thickness of about 1 to 10 nm between two adjacent grain faces show no evidence for a significant corrosive attack.[10,11] This causes even fully corroded $Si_3N_4$ materials to have a residual strength of 400–500 MPa. It was described that silicon nitride materials under certain corrosion conditions exhibit a passivization reaction which blocks the corrosive attack nearly completely.[11–13] This behaviour is strongly connected to the Si–O-structures that partially remain in the corroded triple junctions.

From glass corrosion in acids it is known that network modifying ions are leached completely from the glass structure and corroded layers, consisting mainly of hydrated Si–O-structures, remaining on the surface. At later corrosion stages also these hydrated Si–O-structures dissolve with much slower reaction rates to the

* Corresponding author.
*E-mail address:* jochen.schilm@ikts.fhg.de (J. Schilm).

0955-2219/$ - see front matter © 2003 Elsevier Ltd. All rights reserved.
doi:10.1016/j.jeurceramsoc.2003.07.016

acid.[15,16] This principle corrosion behaviour can be adopted to silicon nitride materials used in this study.[11,13,14]

In contrast the corrosive attack in hydrofluoric acid takes places not only at the triple junctions but also at the above described thin grain boundary films between two adjacent grain faces, which mainly consists of $SiO_2$, and the $Si_3N_4$ grains themselves. The corrosive attack of HF is normally interfacial controlled and does not slow down by a diffusion control or a passivation reaction and finally results in a nearly complete destruction of the material.[2,4,5]

The cited publications indicate that the composition, amount, degree of cristallinity and the distribution of the grain boundary phase severely affect the overall corrosion behaviour. But usually only less attention has been paid to the relations between the composition, especially the silica content of the grain boundary phase, which is mainly responsible for the corrosion resistance in acids.[10,11]

By taking into account that it is not unusual in industry to use acids or caustic solutions that contain impurities, special attention has to be paid to the fluoride ions. Because of their outstanding affinity towards silicon it is assumable that a number of reactions connected with the corrosion process and in which all components (ceramic, aqueous medium, $F^-$ ions) are involved influence each other. This could lead to a change in the corrosion behaviour. The aim of this work was to investigate changes in the corrosion behaviour of $Si_3N_4$ materials with different grain boundary phases due to $F^-$ contaminations in acids.

## 2. Experimental procedure and materials

Silicon nitride ceramics with different compositions (Table 1) were prepared from $Si_3N_4$ powder (Baysinid and UBE SNE 10), $Al_2O_3$ (AKP50), $Y_2O_3$ (grade fine HCST) and $MgAl_2O_4$ (Baykalox). The green samples were produced by mixing the components in an aqueous solution in an attrition mill, spray drying and subsequent cold isostatic pressing at 200 MPa into plates of $6 \times 60 \times 60$ mm$^3$. The organic binder was removed by heat treatment in air. The samples were then sintered in a gas pressure sintering furnace at 1825 °C. From the as sintered plates bending bars with the dimension of $3.0 \times 3.0 \times 45$ mm$^3$ were cut and than grinded.

A deviant procedure was applied to the materials listed in Table 2. The raw powders were suspended in isopropanol and mixed in an attrition mill (Fa. Getzmann) for 4 hours. The powders were dried in a rotavap and granulated using a 400-μm sieve. Bodies of about 100 g ($20 \times 20 \times 70$ mm) were formed by cold isostatic pressing (250 MPa). The samples were gas-pressure sintered at 1825 °C to a density of >99.5% of the theoretical density, and after sintering they were cut and ground into slabs having dimensions of $16 \times 16 \times 2.5$ mm. These samples were then used for corrosion testing.

The as sintered materials were examined by XRD and FESEM neither showing cristallisation of additional oxides or oxynitrides nor demixing phenomena of the completely amorphous grain boundary phase. Compositions of the grain boundary phases were calculated from the raw materials by taking the initial silica content of $Si_3N_4$ powders and the composition of the $Si_{(6-z)}Al_zO_zN_{(8-z)}$ grains into account. The z-values of the $Si_{(6-z)}Al_zO_zN_{(8-z)}$ grains were determined by XRD.[17,18]

All corrosion tests were carried out in a 1.5-l PTFE reaction vessel equipped with sample holders made of Polypropylene (PP) in 1 N $H_2SO_4$ at 90 °C. Earlier results and data from the literature[3,5] have shown that diluted acids with a concentration of about 1 N are highly corrosive for the silicon nitride ceramics of interest, therefore this concentration was chosen. The ratio between the surface of the samples and the volume of the acid was lower than 0.005 m$^{-1}$. All samples were immersed in the corrosive solution for a period of 100h. An exception was made for the kinetic studies on the materials YAl–SiN3 and YAl–SiN7, which last about 260 h. To avoid an enrichment of leached components at the surface of the samples, the solution was continuously stirred. A Lauda thermostat filled with silicone oil was used to heat the vessel. The desired temperature was maintained within a range of ±0.5 K and to measure the mass loss of the dried samples (2h at 150 °C) a balance with an accuracy of ±10 μg was used. The thickness of the corroded layers were investigated microscopically and determined by quantitative image analysis (Image Tool v2). SEM and EDX measurements were conducted to investigate the composition and the

Table 1
Composition of the grain boundary phases of the investigated materials YAl–SiN and MgYAl–SiN calculated from the composition of the raw materials and $z$-values of the $Si_{(6-z)}Al_zO_zN_{(8-z)}$ grains

| Material | Amount of GBP (wt.%) | $SiO_2$ (wt.%) | $Y_2O_3$ (wt.%) | $Al_2O_3$ (wt.%) | MgO (wt.%) | $Si_3N_4$ (wt.%) |
|---|---|---|---|---|---|---|
| YAl–SiN1 (Baysinid) | 10.2 | 2.7 | 6.0 | 1.5 | – | 0.5 |
| YAl–SiN2 (UBE-SNE 10) | 9.8 | 2.7 | 6.0 | 1.1 | – | 0.5 |
| MgYAl–SiN1 (Baysinid) | 5.0 | 2.9 | 1.3 | 0.1 | 0.7 | 0.3 |
| MgYAl–SiN2 (UBE-SNE10) | 4.0 | 2.9 | 0.7 | <0.1 | 0.4 | 0.2 |

Table 2
Composition of the grain boundary phases of the investigated materials YAl–SiN-3 to YAl–SiN-7 calculated from the compositions of the raw materials and $z$-values of the $Si_{(6-z)}Al_zO_zN_{(8-z)}$ grains

| Material | Amount of GBP (wt.%) | $SiO_2$ (wt.%) | $Y_2O_3$ (wt.%) | $Al_2O_3$ (wt.%) | $Si_3N_4$ (wt.%) |
|---|---|---|---|---|---|
| YAl–SiN3 | 12.4 | 4.2 | 6.0 | 1.6 | 0.6 |
| YAl–SiN4 | 12.9 | 4.6 | 6.0 | 1.7 | 0.6 |
| YAl–SiN5 | 13.6 | 5.1 | 6.0 | 1.8 | 0.7 |
| YAl–SiN6 | 14.1 | 5.6 | 6.0 | 1.8 | 0.7 |
| YAl–SiN7 | 9.5 | 4.7 | 4.0 | 0.3 | 0.5 |

morphology of the corroded phases. Strength and residual strength were determined by four point bending (40/20 fixures) on bending bars with the dimensions of 3 × 3 × 50 mm.

## 3. Results

### 3.1. Influence of the fluoride content of the acid

YAl–SiN1, YAl–SiN2, MgAlY–SiN1 and MgAlY–SiN2 were used for the investigation of the influence of the fluoride ion content on the corrosion. A number of experiments were conducted adding increasing amounts of KF (0.01, 0.1 and 1.0 wt.%) to the sulphuric acid and with pure 1N sulphuric acid.

The measured mass losses and thickness of the corrosion layers presented in the Fig. 1 show opposite results for the two YAl–SiN and the two MgAlY–SiN materials. The overall corrosion intensity of the YAl–SiN samples decreases by a factor of 10 when 1.0 wt.% of KF is added to 1N $H_2SO_4$. In contrast the corrosive attack on the MgAlY–SiN materials increases by several orders of magnitude with an increasing amount of KF in the acid. The results received from mass loss data and the corrosion layer thicknesses showed the same tendencies (Fig. 1). SEM micrographs of a corrosion layer of YAl–SiN1 corroded with an amount of 1.0% KF in Fig. 2a–2c show the formation of two sub layers characterized by different levels of porosities. The porosity in the outer corroded layer was larger than that in the inner layer. Fig. 2d shows EDX analyses from the corroded layers and the non corroded $Si_3N_4$ bulk structure. From similar investigations it is reported that yttrium is leached completely from the grain boundary phases by fluoride free acidic solutions and cannot be detected inside the corroded layers by EDX.[11,12] In our case yttrium and fluoride were clearly detected in the inner corrosion layer. These results indicate that $YF_3$ precipitated in the corroded structure. Furthermore, the EDX spectra show a strong reduction of the oxygen signal from the corroded layers. The intensity of the aluminium signal in the corroded layers shows only half of the intensity measured in the non corroded structure.

The materials MgAlY–SiN1 and MgAlY–SiN2 behave in the opposite to the YAl–SiN materials. Up to an addition of 0.01% KF to the acid corrosion layers with thicknesses $<10$ μm were found. The MgAlY–SiN1 sample corroded in the acid having 1.0 wt.% of KF formed two corroded sub-layers which can be distinguished by different porosity levels. SEM pictures of this sample are presented in Fig. 3a–c the corresponding EDX-spectra are given in Fig. 3d. The comparison of the spectra shows that magnesium is detected only in the non-corroded bulk and disappears completely in the

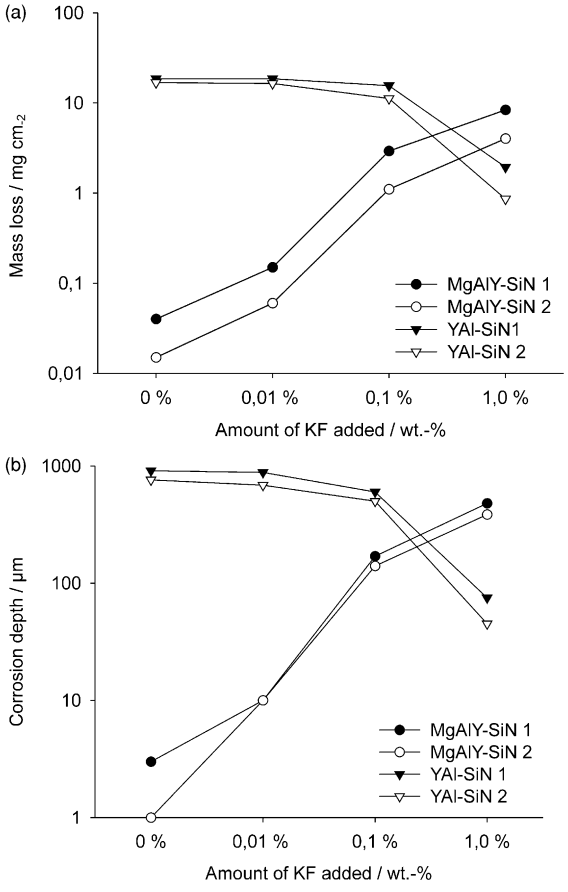


Fig. 1. Mass losses (a) and corrosion depth (b) of the materials YAl–SiN1, YAl–SiN2, MgYAl–SiN1 and MgAlY–SiN2 corroded in 1 N $H_2SO_4$ at 90 °C for 100 h with different amounts of KF added to the acid.

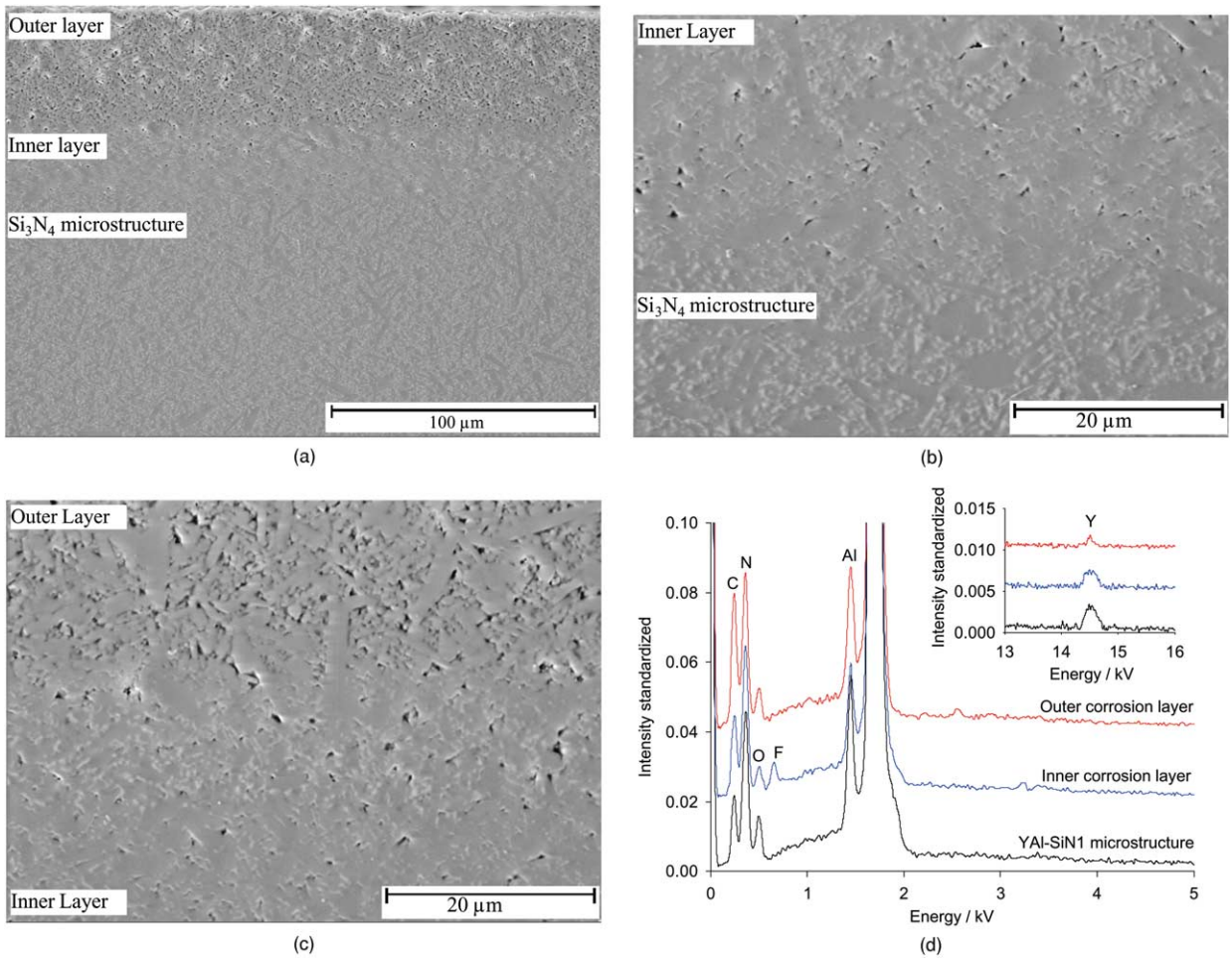


Fig. 2. SEM micrographs of YAl–SiN1 corroded with 1.0 wt.% of KF added; (a) overview; (b) inner corrosion layer and $Si_3N_4$ microstructure; (c) outer and inner corrosion layer; and (d) EDX spectra of the corrosion layers and the $Si_3N_4$ microstructure of YAl–SiN1; important peaks are labelled with the letters of the corresponding elements. (C was used for the coating.)

corroded layers. The concentration of aluminium in the corroded areas is reduced significantly compared to that of the non corroded material.

The residual strength of the materials YAl–SiN2 and MgAlY–SiN2 are presented in Fig. 4. Independently on the amount of KF added to the acid the residual strength of YAl–SiN2 was reduced to a constant level in the range of 550–500 MPa in comparison to the initial strength. In contrast MgAlY–SiN2 showed a clear dependence of the residual strength on the KF concentration in the corrosive medium. Without any KF additions only a slight reduction of the strength was observed. With increasing concentration of KF in the acid the strength reduces continuously to a lower value in comparison to material YAl–SiN2.

### 3.2. Influence of the $SiO_2$-content of the grain boundary phase on the corrosion

Five materials denoted as YAl–SiN3 to 7 (Table 2) with varying $SiO_2$ contents in the grain boundary phase were used for the investigations on the influence of the composition of the grain boundary phase. It must be remarked that the alumina and yttria contents in the grain boundary phase of the material YAl–SiN7 are reduced by 33 wt.% compared to the other materials. But due to the high silica content, which governs the corrosion resistance of YAl–SiN7 in acidic environments, the reduced additive content has only an inferior influence on the corrosion behaviour.[13] Two sets of experiments, one with KF free 1 N sulphuric acid and one with 1.0 wt.% of KF added to the acid, were carried out. Fig. 5 presents the mass loss data and the thickness of the corrosion layer. The results show that an increased $SiO_2$ content in the grain boundary phase lead to strongly improved corrosion resistance in pure 1N $H_2SO_4$. In contrast the corrosion in 1 N $H_2SO_4$ with an addition of 1.0% of KF showed the opposite dependence on the $SiO_2$ content in the grain boundary phase.

Up to now the situation of the corrosion behaviour within a time range of 100 h has been described. Fig. 6 shows the results of a kinetic study conducted with

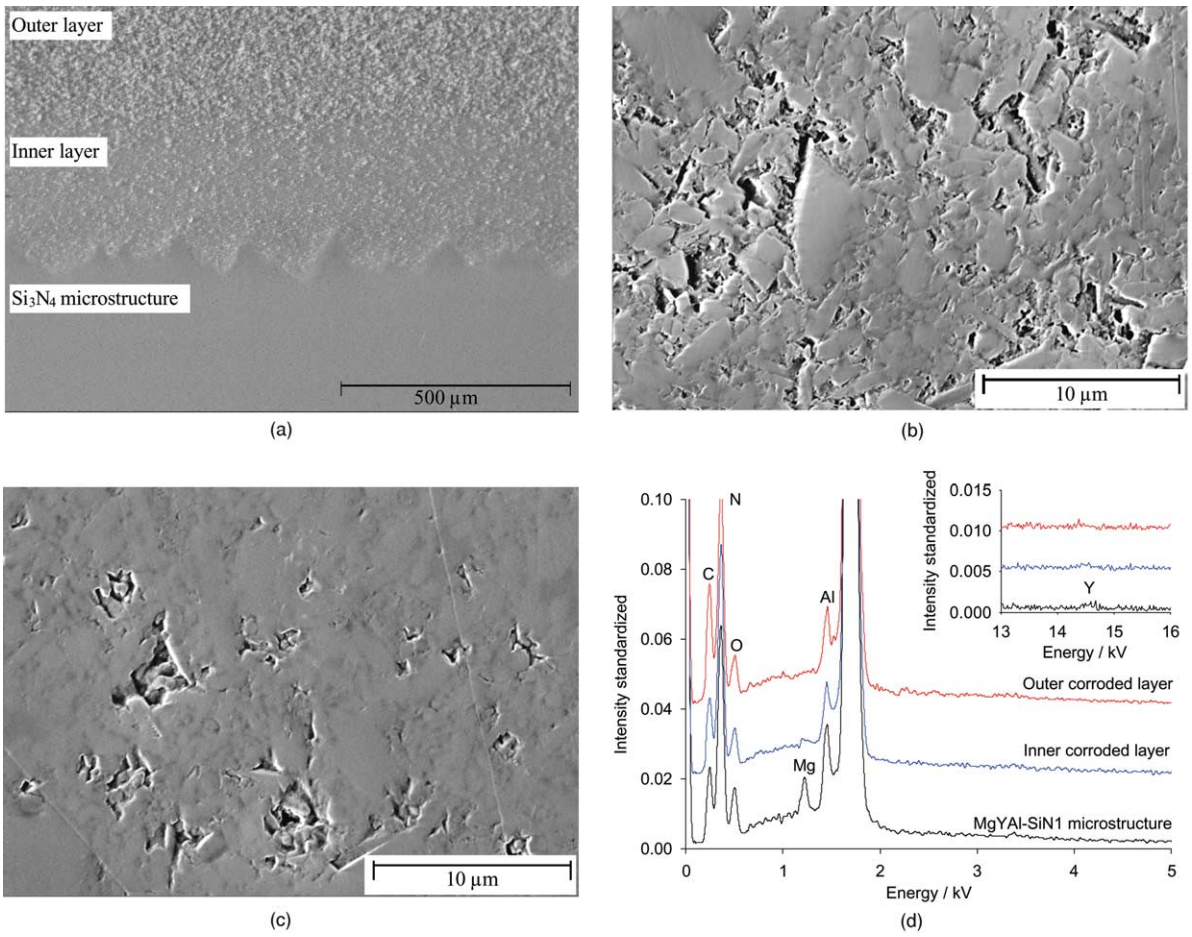


Fig. 3. SEM micrographs of MgYAl–SiN1 corroded with 1.0 wt.% of KF added; (a) overview; (b) outer corrosion layer; (c) inner corrosion layer; and (d) EDX spectra of the corrosion layers and the $Si_3N_4$ microstructure of MgYAl–SiN1; important peaks are labelled with the letters of the corresponding elements (C was used for coating).

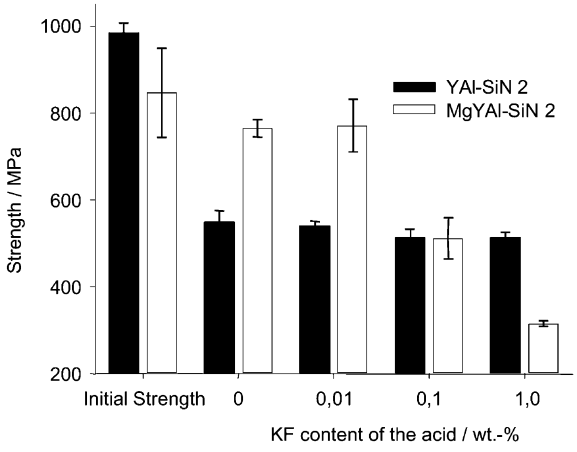


Fig. 4. Initial and residual strength of YAl–SiN2 and MgAlY–SiN2 corroded in 1N $H_2SO_4$ with different amounts of KF at 90 °C after 100 h.

YAl–SiN3 and YAl–SiN7 in 1N sulphuric acid with and without 1.0% of KF. While YAl–SiN3 shows a more complex behaviour in the additive-free acid, which is in detail described by Schilm et al.,[13] the corrosive attack of YAl–SiN7 proceeds linearly with time. The addition of 1.0% KF causes both materials to corrode within the first 100 hours in a linear manner. For longer corrosion times in KF containing solutions no passivization was found as for KF free corrosion of YAl–SiN3. The opposite takes place. A slight but continuous acceleration of the reaction can be observed. A closer examination of the samples corroded for 260 h showed that the grains at surface were only loosely attached and could be removed easily.

Additionally the cross sections of YAl–SiN3 and YAl–SiN7 were observed by using SEM. For example in Fig. 7 the material YAl–SiN3 is shown. The corrosion layers formed under different conditions point up the destructive influence of the KF additives. The sample corroded without KF addition in the acid in the Fig. 7a and b was polished. The sample corroded with KF addition showed a weak corrosion layer. Therefore this sample was not polished for analysis. Results of our SEM investigations reveal that in KF free acid two corrosion sub layers with different porosities are formed (Fig. 7a and b). An even higher porosity is observed in

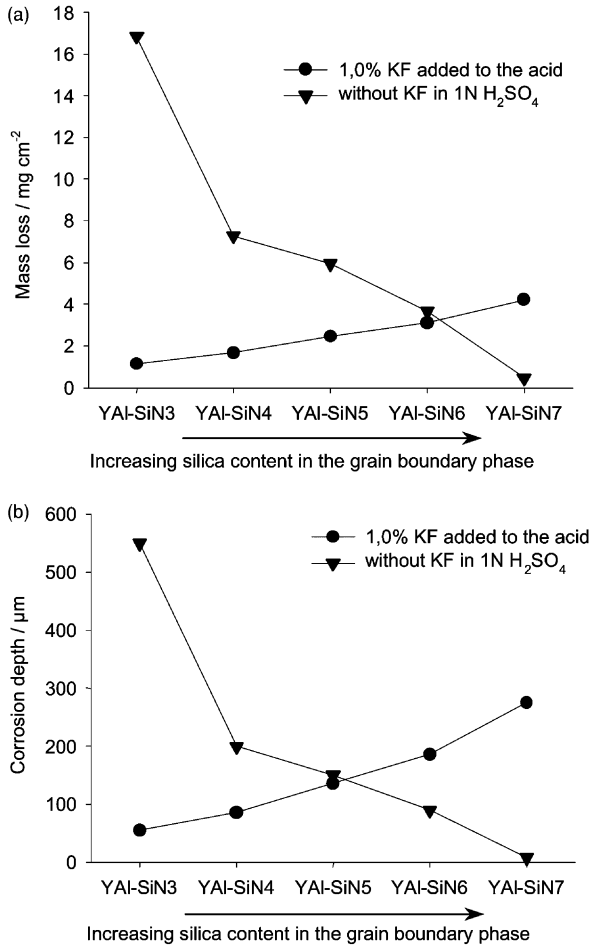


Fig. 5. Mass loss data (a) and corrosion depth (b) of the materials YAl–SiN3 to YAl–SiN7 after corrosion in 1N $H_2SO_4$ with and without 1.0 wt.% of KF added after 100 h at 90 °C.

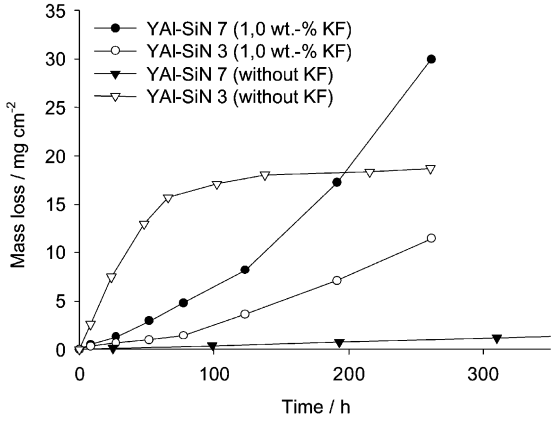


Fig. 6. Time dependent mass loss data of YAl–SiN3 and YAl–SiN7 in 1N $H_2SO_4$ containing 1.0 wt.% KF and KF free acid at 90 °C.

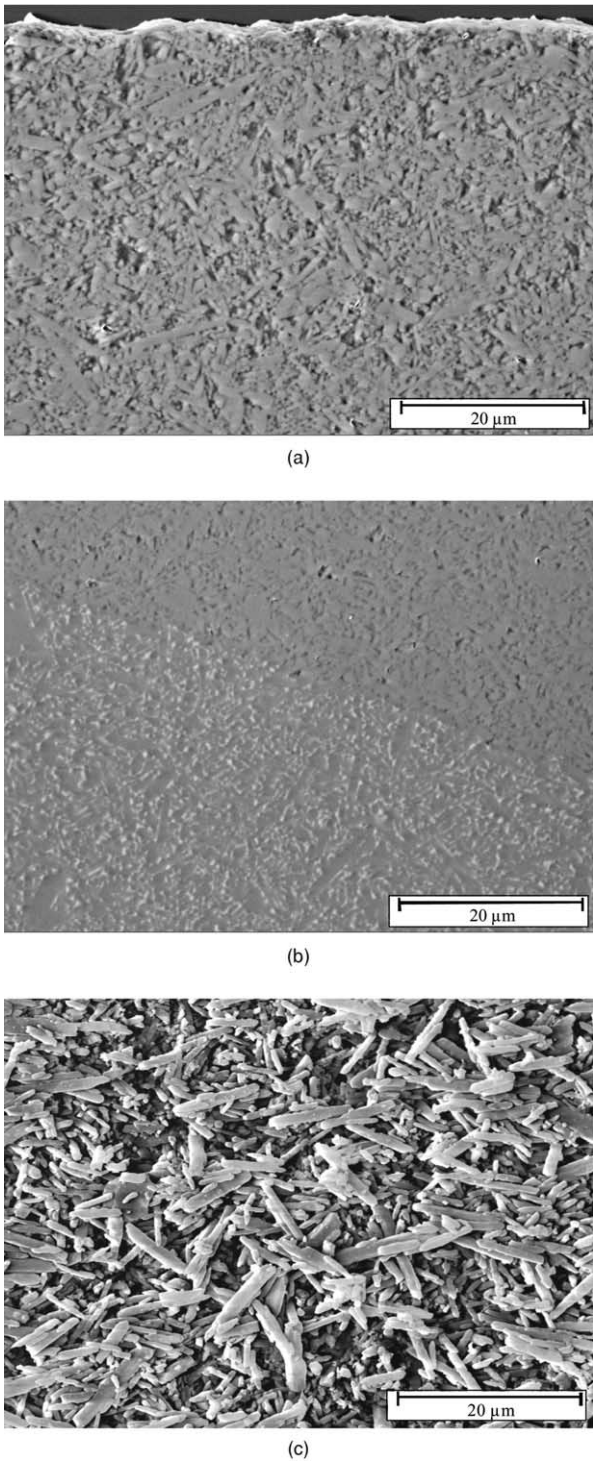


Fig. 7. SEM micrographs of YAl–SiN3 corroded under different conditions; (a) 216 h in 1N $H_2SO_4$ at 90 °C without any KF added; outer region of the corroded layer (polished cross section); (b) Conditions as in (a) inner region of the corrosion layer (polished cross section); and (c) corrosion layer after 260 h in 1N $H_2SO_4$ at 90 °C with 1.0 wt.% KF added (cross section as cut).

the case of the material corroded in KF containing acid (Fig. 7c). Prolonged corrosion times continue the destruction process, which leads to a loose network of $Si_3N_4$ grains. After 260 h of a corrosive attack in the KF containing acid the corrosion layer can be characterized by a high porosity level and spalled grains. Also no different porosity levels are observed inside the corroded layer of this sample.

Also several EDX analyses, which are presented in Fig. 8, were carried out on the corroded samples of YAl–SiN3. The corrosion in KF free acid causes the complete leaching of yttrium from the grain boundary phase (Fig. 8a). A comparison of the EDX spectra in Fig. 8a shows a higher oxygen content in the inner corroded layer than in the outer corroded layer. Different results were obtained from the samples corroded in 1.0% KF containing acid. After 100 h of corrosion YAl–SiN3 shows the appearance of only one thin corrosion layer with a thickness of about 50μm. The EDX analysis of this sample in Fig. 8b indicated a considerable reduction of the oxygen content in the corrosion layer. Also clear signals of yttrium and fluoride could be detected in this layer. In all cases aluminium was leached only partially due to the incorporation of Al into the $Si_3N_4$ lattice during sintering resulting in insoluble $\beta$–$Si_{(6-z)}Al_zO_{(8-z)}N_z$ ($z < 0.34$) grains.[17,18]

## 4. Discussion

The reasons for the different corrosion behaviour of the YAl–SiN and MgYAl–SiN materials presented in Section 3.1 are mainly connected with the composition of their grain boundary phases and complex interactions with the sulphuric acid and the fluoride ions. This meets also for the series of YAl–SiN materials. The flow chart in Fig. 9 gives a possible explanation. Without $F^-$ ions the network modifying ions like $Y^{3+}$, $Al^{3+}$ and $Mg^{2+}$ are leached from the grain boundary phase. A highly hydrated Si–O-structure remains inside the corroded triple junctions. This behaviour is supported by the EDX analyses of the inner corrosion layer in Fig. 8a. The Oxygen content in the inner layer is a strong hint for residual hydrated silica structures. These structures are hardly detectable in a direct manner due to their small amount inside the corroded triple junctions and their amorphous character. During the corrosion process a condensation reaction occurs, which stabilises these structures.[13] These reactions are similar to the condensation of a $SiO_2$ gel. This dense Si–O-network acts as a transport barrier for the leached network modifiers and let the corrosion process stop nearly completely. It has been demonstrated in literature that materials with a high $SiO_2$ content in the grain boundary phase (as MgAlY–SiN1, 2 and YAl–SiN7) are more stable in acids than materials with a low $SiO_2$ content (as YAl–SiN1 and 2) (Figs. 1 and5) are.[10,11]

The Fluoride ions participate in the corrosion processes in two ways (Fig. 9). On the one hand they are able to form $[SiF_6]^{2-}$ complexes with silicon which results in a further dissolution of the Si–O-network and forces the overall corrosion intensity. The occurence of this reaction is supported by the strong enhancement of corrosion of the MgYAl–SiN material in KF containing acid. On the other hand fluoride can form insoluble $YF_3$ with the leached $Y^{3+}$-ions inside the corroded structure. This behaviour has been reported in other studies where $Si_3N_4$ materials were corroded in hydrofluoric acid at various concentrations.[2,4–6] The $YF_3$ precipitates in the triple junctions and forms a transport barrier. This causes a strong slowing down of the corrosion process (Figs. 1, 2 and 6). The amount of solid $YF_3$ produced in the corroded material depends on the concentration of

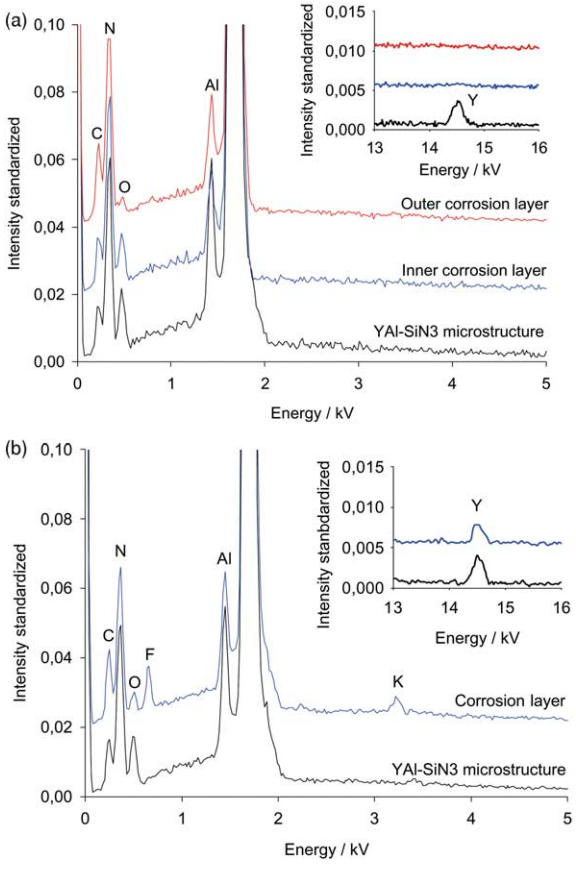


Fig. 8. EDX spectra of YAl–SiN3 corroded under different conditions; important peaks are labelled with the letters of the corresponding elements; (a) after 216 h in 1N $H_2SO_4$ at 90 °C without any KF added; (b) after 100 h in 1N $H_2SO_4$ at 90 °C with 1.0 wt.% KF added.

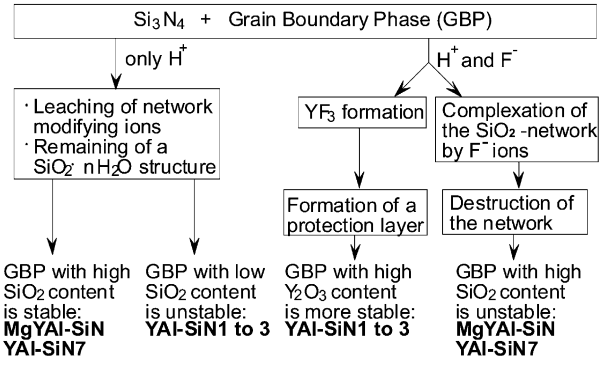


Fig. 9. Schematic flow of the processes during corrosion on $Si_3N_4$ in acids with and without the influence of fluoride.

KF added to the acid. And therefore a decrease of the corrosion of the YAl–SiN samples is observed caused by the formation of the $YF_3$-passivization layer. This compensates the destruction of the Si–O-network partially due to the fluoride ions. In contrast to the materials YAl–SiN1 and YAl–SiN2 the MgYAl–SiN1 and MgYAl–SiN2 samples show a complete different dependence of the corrosion behaviour on the amount of KF added. In the MgYAl–SiN1 and 2 materials that have a low Y content and a high $SiO_2$ content in the grain boundary phase (Table 1), the increasing destruction of the Si–O-network with increasing KF concentration is the decisive process. A comparison of the EDX spectra in Fig. 3d reveals that in the corroded structures neither fluoride nor yttrium were detected. Again the oxygen content in the corroded layer can be explained by the formation of SiAlON-grains during the sintering process. These implementations are supported by the Figs. 2 and 3. The residual strength of MgAlY–SiN2 decreases with increasing KF content while the strength of YAl–SiN2 remains within a certain range independently of the KF content (Fig. 4). This indicates that the $SiO_2$-rich phase in MgAlY–SiN2 is increasingly attacked by the fluoride ions within 100 h of corrosion. Even a concentration of 0.01 wt.% of KF in the acid let the corrosion intensity of MgYAl–SiN1 increase up to 3 times under the applied conditions (Fig. 1). In KF free acid there is no significant destruction of the $Si_3N_4$ microstructure and a corrosion depth of less than 10 μm is measured. There is no evidence for a remarkable dissolution of the $Si_3N_4$ grains within the first 100 h of a corrosive attack.[10] The fact, that only one half of the aluminium is dissolved to the acid can be explained by the incorporation of some aluminium into the grains.[15,16] This incorporated fraction cannot be leached by the acid under the applied corrosion conditions.

The occurrence of several corrosion layers with different porosity levels in the tested materials has recently been described for $Si_3N_4$ ceramics containing a $Y_2O_3$–$Al_2O_3$–$SiO_2$-glass as a grain boundary phase.[12,13] In all cases, the outer corroded layer exhibits a larger porosity than the inner layer does. It is probable that the leaching process of network changing ions ($Mg^{2+}$, $Y^{3+}$, $Al^{3+}$) and their transport through the corrosion layer occurs faster than the dissolution of the remaining $SiO_2$-network in the triple junctions. This corrosion behaviour is also known from silicate glasses.[15,16]

As mentioned before, the $SiO_2$ content of the grain boundary phase is a governing factor concerning the corrosion stability in acidic media.[13] In fluoride ion free acids a high amount of $SiO_2$ in the grain boundary phase results in a high stability, whereas in fluoride ions containing acids the $SiO_2$ glass network is not stable (Fig. 5). At lower $SiO_2$ concentrations in the grain boundary phase and high contents of yttria a $YF_3$ barrier inside the corroded layer dominates the corrosion process and reduces the intensive leaching of the grain boundary phase that is observed in fluoride free acid (YAl–SiN3 and 4). With an increasing $SiO_2$ content the opposed processes of leaching and complexing of silica on the one hand and precipitating of $YF_3$ on the other hand partially compensate each other (YAl–SiN 5 and 6). This ends in a situation in which the destruction of the microstructure by fluroide dominates the entire process (YAl–SiN 7).

At longer corrosion times (> 100 h) the destructive effect of the fluoride ions is also in materials with lower $SiO_2$ contents more pronounced. An accelerated corrosion rate and no passivization was observed (Fig. 6). Starting at the outer interface the thin grain boundary films dissolve and a weak outer corroded layer with loosely attached $Si_3N_4$ grains is formed (Figs. 7c).

## 5. Conclusions

It was shown that the corrosion resistance of different silicon nitride materials in 1 N $H_2SO_4$ acidic solutions containing fluoride is highly sensitive to the composition of the grain boundary phase. A material containing a high amount of yttria in the grain boundary phase is able to produce insoluble $YF_3$ which is deposited in the corroded triple junctions and inhibits the corrosion process. On the other side materials containing a lower amount of yttria and a higher $SiO_2$ content in the grain boundary phase undergo an intensive corrosive attack due to the dissolution of the protective $SiO_2$-network by the $F^-$ ions. This behaviour is inverse to that in fluoride free acids. Prolonged corrosion times in fluoride containing $H_2SO_4$ result in a complete destruction of the microstructure and the formation of a weak corrosion layer.

## Acknowledgements

This work was supported by the AIF under contract number 12130 BR

## References

1. Sato, T., Tokunaga, Y., Endo, T., Shimada, M., Komeya, K., Kameda, T. and Komatsu, M., Corrosion of silicon nitride ceramics in aqueous hydrogen chloride solutions. *J. Am. Ceram. Soc.*, 1988, **71**(12), 1074–1079.
2. Sato, T., Tokunaga, Y., Endo, T., Shimada, M., Komeya, K., Komatsu, M. and Kameda, T., Corrosion of silicon nitride ceramics in aqueous HF solutions. *J. Mat. Sci.*, 1988, **23**, 3440–3446.
3. Iio, S., Okada, A., Asano, T. and Yoshimura, M., Corrosion behaviour of silicon nitride ceramics in aqueous solutions (Part 3). *J. Ceram. Soc. Japan, Int. Edition*, 1992, **100**, 954–957.
4. Shimada, M. and Sato, T., Corrosion of silicon nitride ceramics

in HF and HCl solutions. *Ceram. Trans. Symp*, 1990, **10**, 355–365.
5. Sharkawy, S. W. and El-Aslabi, A. M., Corrosion of silicon nitride ceramics in aqueous HCl and HF solutions at 27 °C – 80 °C. *Corrosion Science*, 1998, **40**(7), 1119–1129.
6. Bellosi, A., Graziani, T. and Monteverde, F., Degradation behaviour of silicon nitride in aqueous acid solutions. *Key Engin. Mat*., 1996, **113**, 215–226.
7. Kanbara, K., Uchida, N., Uematsu, K., Kurita, T., Yoshimoto, K. and Suzuki, Y., Corrosion of silicon nitride ceramics by nitric acid. *Mat. Res. Soc. Symp. Proc*., 1993, **287**, 533–538.
8. Okada, A. and Yoshimura, M., Mechanical degradation of Silicon nitride ceramics in corrosive solution of boiling sulphuric acid. *Key Engin. Mat*., 1996, **113**, 227–236.
9. Monteferde, F., Mingazzini, C., Giorgi, M. and Bellosi, A., Corrosion of silicon nitride in sulphuric acid aqueous solution. *Corrosion Science*, 2001, **43**, 1851–1863.
10. Herrmann, M., Klemm, H. and Schubert, C., Silicon Nitride Materials. In *Handbook of Ceramic Hard Materials, Vol. 2*, ed. R. Riedel. WILEY-VCH Verlag GmbH, D-69469, Weinheim, 2000, pp. 749–801.
11. Herrmann, M., Schilm, J., Michael, G., Meinhardt, J. and Flegler, R., Corrosion of Silicon Nitride materials in acidic and basic solutions and under hydrothermal conditions. *J. Eur. Ceram. Soc*., 2003, **23**, 585–594.
12. Seipel, B. and Nickel, K. G., Corrosion of silicon nitride in acidic solutions: penetration monitoring. *J. Eur. Ceram. Soc*., 2003, **23**, 595–602.
13. Schilm, J., Herrmann, M. and Michael, G., Kinetic study of the corrosion of silicon nitride materials in acids. *J. Eur. Ceram. Soc*., 2003, **23**, 577–584.
14. Herrmann, M., Amercian Ceramic Society, Annual Meeting 2002.
15. Grambow, B. and Mueller, R., Firts-order dissolution rate law and the role of surface layers in glass perfomance assessment. *J. of Nuc. Mat., (298)*, 2001, 112–124.
16. Scholze, H., *Glas Natur, Struktur, Eigenschaften*. Spinger-Verlag, Heidelberg, 3. Aufl, 1988.
17. Riedel, G., Bestgen, H. and Herrmann, M., Influence of sintering additives with differing proportions of $Y_2O_3/Al_2O_3$ on the sintering and material properties of $Si_3N_4$ ceramics. *cfi / Ber. DKG*, 1998, **75**(10), 30–34.
18. Riedel, G., Bestgen, H. and Herrmann, M., Correlation between structure ans properties of $Si_3N_4$ materials with $Y_2O_3/Al_2O_3$ sintering additives. *cfi / Ber. DKG*, 1999, **76**(1-2), 24–27.